

Performance of UWB Array-Based Radar Sensor in a Multi-Sensor Vehicle-Based Suit for Landmine Detection

Alexander Yarovoy^{#1}, Timofey Savelyev[#], Xiaodong Zhuge[#], Pascal Aubry[#], Leo Lighthart[#],
John Schavemaker^{*}, Peter Tettelaar^{*}, Eric den Breejen^{*2}

[#]*IRCTR, Delft University of Technology,
Mekelweg 4, 2628CD Delft, The Netherlands*

¹*a.yarovoy@irctr.tudelft.nl*

^{*}*TNO Defence, Security, and Safety,*

The Hague, The Netherlands

²*eric.denbreejen@tno.nl*

Abstract - In this paper, integration of an UWB array-based time-domain radar sensor in a vehicle-mounted multi-sensor system for landmine detection is described. Dedicated real-time signal processing algorithms are developed to compute the radar sensor confidence map which is used for sensor fusion. Performance of developed algorithms for stand-alone GPR sensor and multi-sensor suit is verified experimentally.

INTRODUCTION

It has been demonstrated that GPR is a useful sensor for multi-sensor system dedicated to landmine detection, especially for humanitarian demining [1]. Numerous field trials of different GPR sensors have proven that while for most ground types, GPR sensor can achieve desirable detectability level, a decrease of the false alarm rate remains the most important task for GPR developers. This decrease can be achieved by combination with other sensors like metal detector and Electro Optic camera. In fusion research we assume that GPR should be a leading sensor for buried objects while Electro Optic camera should lead for surface-laid objects. Metal detector should verify if there is any metal content in the objects detected by camera or GPR. Performance of the whole multi-sensor suit depends very much on the way how information from different sensors is fused.

For a number of years TNO Defence, Security and Safety investigates capabilities of sensor fusion for landmine detection [2]. TNO has developed a multi-sensor test platform to test the capabilities of sensors in real-time operation on a multi-sensor system (Fig. 1). The system has to scan ground with a speed of at least 2km/h. Such operational speed is too high for conventional GPR based on sequential data acquisition. Thus it has been decided to use a newly developed in IRCTR multi-channel UWB sensor with digital footprint forming [3]. This radar can support the scanning speed up to 148km/h due to its innovative system design. However, realization of real-time data processing for this system remains a challenge. This paper describes developments of such real-

time processing scheme and experimental verification of its performance.



Fig. 1. TNO multi-sensor test trolley for landmine detection research

The paper is organized in the following way. IRCTR radar is briefly described in Section II. Embedding of the radar in the multi-sensor suit is discussed in Section III. Dedicated signal processing scheme is presented in Section IV. Performance of the signal processing scheme (stand alone and integrated in multi-sensor system) is described in Section V. Main outputs of the work are summarized in Section VI.

ARRAY-BASED UWB RADAR SENSOR

IRCTR mini-array GPR comprises a pulse generator, an antenna array system, a seven-channel signal conditioner and an eight-channel sampling converter. A block scheme of a mini-array radar is shown in Fig. 2.

The generator fires a step pulse with a rise time of about 90ps. Such a waveform improves radar power budget at low frequencies, which are not efficiently radiated by the transmit antenna due to a relatively small size of its physical aperture. The receiver chain consists of a seven-channel signal condi-

tioner and an eight-channel sampling converter (built by Geo-Zondas Ltd., Lithuania). The receiver chain has an analog bandwidth from 200MHz up to 6GHz and the linear dynamic range of 69dB (with averaging over 128 samples). The sampling converter operates with the sampling rate of 500kHz per channel. Observation time window can be varied from 32ps till 20ns with a number of acquisition points available from 16 till 4096. Large flexibility in duration of the observation time window and the sampling time allows us to adjust the system to different ground types and data acquisition scenarios. A very important feature of the sampling converter is its high measurement accuracy. The maximal error in the amplitude scale and the time scale linearity of the sampling converter is of about 1%.

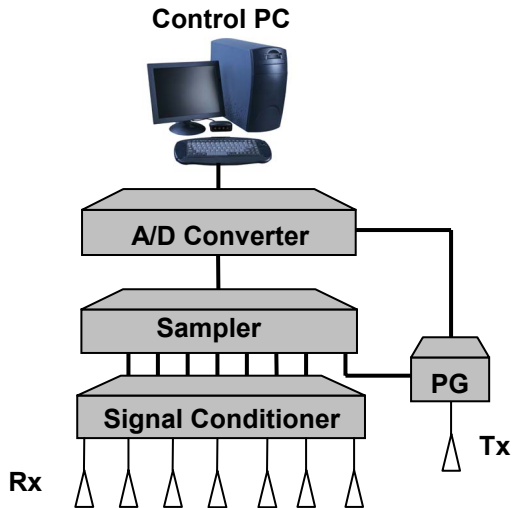


Fig. 2 Block scheme of IRCTR radar

An important part of the receiver chain is the signal conditioner. The signal conditioner improves the signal to noise ratio and allows to use the whole dynamic range of the ADC. The equivalent noise floor (which includes the quantization noise of ADC) of the receiver is less than 1.5mV RMS without averaging. The spectrum of the noise corresponds to the almost white noise so it can be efficiently suppressed by averaging. The signal conditioner decreases the noise floor and improves the signal-to-noise ratio by almost 30dB.

The long-term stability of the radar is characterized by the time-delay drift of about 12ps/hour. To improve the long term stability of the system the eighth channel of the sampling scope is used. This channel acquires one of two signals. For the time axis calibration a 4GHz harmonic signal from the internal generator of the sampling scope is acquired. For the delay drift compensation the reference signals from the generator is acquired. The data post-processing is used for compensation of the time drift based on the reference signals acquired in the eighth channel. As a result of this compensation, the time drift less than 1ps/hour has been achieved.

The radar antenna system consists of a single transmit antenna elevated 60cm above the ground and a linear array of the

receive antennas (loops) elevated 20cm above the ground. The whole antenna system is mounted on the TNO test platform and covered with a protective shield (Fig. 3).



Fig. 3 Antenna system of the radar mounted at the TNO test platform

RADAR EMBEDDING IN MULTI-SENSOR SUIT

Schematics of the multi-sensor system is given in Fig. 4. The data acquisition and transfer is synchronized by means of a tick wheel mounted on the vehicle. The wheel sends a TTL pulse via RS232 to the sensor units and fusion processor at given intervals (2.5cm). The GPR sensor unit acquires and processes a B-scan when triggered by the tick wheel; it stores the raw and/or pre-processed data and transfers it through TCP/IP to the fusion processor on request.

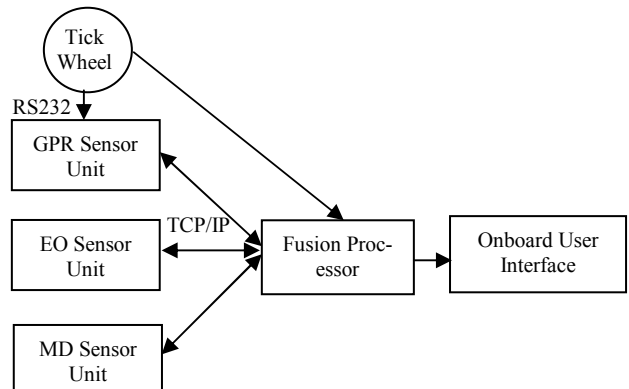


Fig. 4 Schematics of the multi-sensor suit

RADAR SIGNAL PROCESSING

Standard processing scheme includes background subtraction, subsurface imaging and confidence map computation. Second step is the most time consuming one and typically is realized only in off-line processing. However both detectability and correct positioning of subsurface targets can be essentially improved by adding subsurface imaging into the processing chain. Thus a dedicated real-time imaging scheme has been developed and implemented in the system.

Background subtraction is done in two major steps: subtraction of the antenna coupling and moving average subtraction. Size and shape of the moving window has been optimized to fit the geometry of the antenna system and scanning speed. Band pass filter is applied in each A-scan signal in order to suppress uncorrelated noise outside the operational bandwidth.

Imaging scheme is based on the modification of Kirchhoff migration algorithm [4] originated in the field of geophysics. Under near-field conditions, this technique is able to improve both spatial resolution and signal to clutter noise ratio (SCNR) of the survey comparing with conventional synthetic aperture radar (SAR) imaging techniques, such as diffraction stack algorithm. The idea of Kirchhoff migration is to back-propagate the scalar wave front, measured in the data acquisition plane, to the object plane at time zero, using an integral solution to the scalar wave equation. Suppose $u(\mathbf{r}, t)$ represents the received field on the data acquisition plane, the migrated wave field at a point with coordinates \mathbf{r}' can be obtained from the following equation

$$u(\mathbf{r}', t) = \iint (\cos \phi_1 + \cos \phi_2) \frac{1}{v} \frac{\partial}{\partial t} u(\mathbf{r}, t + \frac{R_1 + R_2}{v}) dx dy \Big|_{t=0} \quad (1)$$

where R_1 and R_2 represent the propagation distance between the point to be migrated \mathbf{r}' and the positions of transmit and receive antennas; ϕ_1 and ϕ_2 express the aspect angles between the range direction and respective antennas; v denotes the propagation velocity in the medium.

The feasibility of applying this algorithm to electromagnetic problems lies on the fact that vector wave equations reduce to scalar wave equation in a homogeneous, isotropic medium. The algorithm is based on complete linear operations and therefore can be efficiently implemented. The focusing is performed in both cross-track and along-track directions to provide instant 3D resolution. The obtained images are updated iteratively as the scanning continues. In this way, the computation load can be further spread over time. The refraction effect of air-ground interface is also compensated for better focusing of buried targets. The time delay due to propagating underground is calculated according to Snell's law of refraction us-

ing a Newton-Raphson method, which converges fast within minimum number of iteration.

Confidence maps are computed in the following way. The resulting 3D image is continuously translated into two-dimensional matrixes by using a windowed energy projection as the area under scanning moves outside the footprint of the transmit antenna. Then it is scaled by a background model which is trained as the array response to the minimum detectable target. The resulting confidence map is expressed in logarithmic scale for larger dynamic range and transferred to the fusion computer sequentially within a short latency. The computed confidence map is aligned to the total detection grid of the whole multi-sensor system, which has a size of 2.5cm.

The processing scheme is implemented in the data flow shown in Fig. 5. Here the pre-processed data stored and transferred by the GPR sensor unit are the confidence maps.

GPR sensor

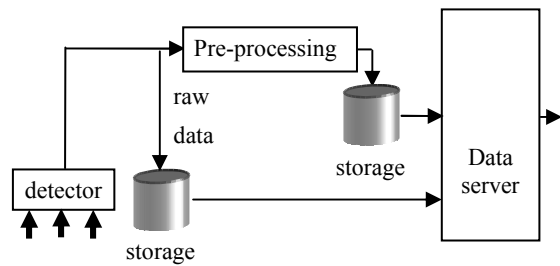


Fig. 5 Data flow in GPR sensor

PROCESSING SCHEME PERFORMANCE

Performance of the developed data processing scheme has been evaluated first in laboratory conditions. The radar has scanned over a number surface laid mines (which is the most difficult for GPR type of targets due to masking of target return by ground bounce). Typical scenario is shown in Fig. 6. The produced confidence map is shown in Fig. 7. It can be seen that the radar efficiently detects and localizes plastic mines. Furthermore, the processing scheme allows separate detection of small targets laid close to large ones.

After that the radar has been tested in quasi-real conditions at premises of TNO. A number of anti-tank and anti-personnel mines as well as typical false alarms have been buried in a grass field. The vehicle was moving with a speed of about 36km/h. No problems with real-time operation of the radar have been detected. The radar was capable to detect all surface-laid and buried mines. An example of radar performance is shown in Figure 8.

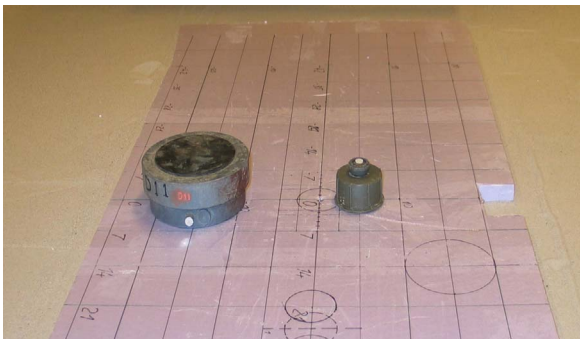


Fig. 6 Typical scenario with two surface laid anti-personnel mines separated by 10cm

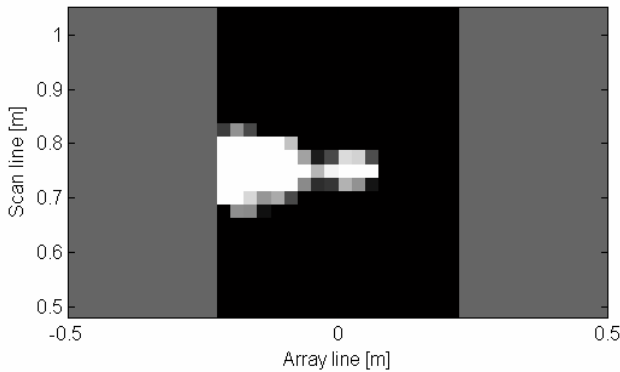


Fig. 7 GPR confidence map for scenario shown in Fig. 6

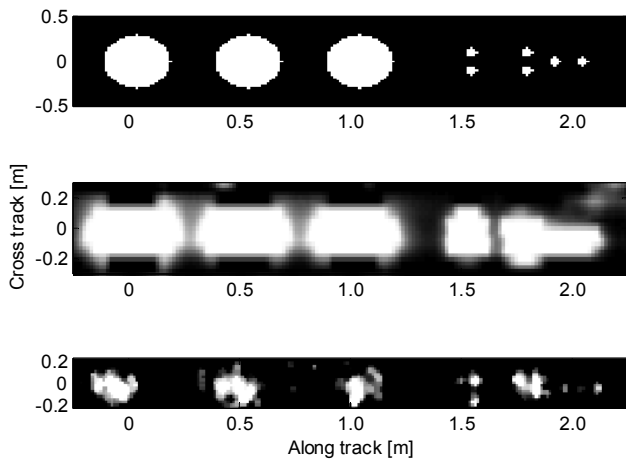


Fig. 8 Scenario with buried anti-tank and anti-personnel mines (top), confidence map of the metal detector (middle) and radar confidence map (bottom)

In the scenario with 3 metal antitank mines buried at a variable depth from 10cm to 20cm and 6 metal anti-personnel mines (some of the were flash-buried, some of them were bur-

ied at a depth of 5cm) the radar has detected all mines as separate targets in proper positions while metal detector was not able to resolve separate anti-personnel mines. A single false alarm (caused by strong surface laid scatterer) has been produced by the radar.

CONCLUSION

Developed in IRCTR UWB array-based time-domain radar sensor has been integrated in a vehicle-mounted multi-sensor system for landmine detection. A dedicated data processing has been developed for real-time operation within the multi-sensor suit. The processing scheme includes background subtraction, subsurface imaging and confidence map computation. Results of the field trials demonstrated reliable detection of anti-tank and anti-personnel mines by vehicle speed of about 36km/h. The radar sensor is also capable to detect and correctly localize small plastic mines (even in a vicinity of strong scatterers). Fusion of radar and metal detector confidence maps will be presented elsewhere.

ACKNOWLEDGMENT

The authors would like to thank P.J. Fritz and A.J. Overtoom (both TNO) for their technical assistance during mechanical integration of the radar into multi-sensor vehicle, system assembling and testing.

This research is partly performed under a contract between TNO Defence, Security and Safety and IRCTR. The TNO activities are part of the Defence research programme V516 Mobility and Counter-mobility.

REFERENCES

- [1] McDonald, J., et al., *Alternatives for landmine detection*, Rand Corporation, 2003.
- [2] J.G.M. Schavermaker, E. Den Breejen, K.W. Benoist, K. Schutte, P. Tettelaar, M. de Bijl, P. J. Fritz, L.H. Cohen, W. van der Mark, and R. J. Chignell, "LOTUS field demonstration of integrated multisensor mine detection system in Bosnia," *Detection and Remediation Technologies for Mines and Minelike Targets VIII, Proc. SPIE*, vol. 5089, 2003, pp. 1324-1335, 2003.
- [3] A.G. Yarovoy, T.G. Savelyev, P.J. Aubry, P.E. Lys, and L.P. Ligthart, "UWB array-based sensor for near-field imaging," *IEEE Transactions on Microwave Theory and Techniques*, vol. 55, pp. 1288-1295, June 2007.
- [4] X. Zhuge, T.G. Savelyev, A.G. Yarovoy, and L.P. Ligthart, "UWB Array-Based Radar Imaging Using Modified Kirchhoff Migration," accepted by *ICUWB 2008*.